

# First Experiments with $e^-/H^-$ Plasmas: Enhanced Centrifugal Separation from Diocotron Mode Damping

A.A. Kabantsev<sup>a)</sup>, K.A. Thompson, and C.F. Driscoll

*Department of Physics, University of California at San Diego, La Jolla, CA 92093-0354, USA*

<sup>a)</sup>Corresponding author: akabantsev@ucsd.edu

**Abstract.** Negative hydrogen ions are produced and contained within a room-temperature electron plasma, by dissociative electron attachment onto excited  $H_2$  neutrals. We observe a strongly enhanced centrifugal separation of electrons and ions when a diocotron mode is present. The outward ion transport rate is proportional to the diocotron mode amplitude, with concurrent diocotron mode damping. This is not yet understood theoretically.

## INTRODUCTION

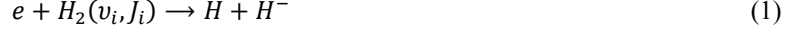
Two-species non-neutral plasmas, such as  $e^-/H^-$ , have the desirable confinement properties expected from conservation of angular momentum; and they also exhibit novel waves, damping, and transport effects due to the disparate masses. Here, we describe the apparent enhancement of centrifugal mass separation driven by 2-species diocotron mode dynamics, inviting theory analysis.

In the case of multispecies plasmas confined in the Penning-Malmberg trap, an important feature is that the plasma (as the electrons cool down radiatively with  $e$ -folding time  $\tau_c = 386 \text{ sec}/B_{kG}^2$ ) relaxes towards a thermal equilibrium characterized by a centrifugal separation between the components of different masses [1] with heavy species pushed to the outside of the plasma. The degree of separation depends on the ratio between the difference in centrifugal potentials for each species and the plasma thermal energy  $k_B T$ . Due to the mass difference, the rotation frequencies  $\omega_R$  are never the same (before reaching thermal equilibrium), so there is a collisional drag between the species as the basic separation mechanism. This drag force  $F\hat{\theta}$  produces a  $F \times B$  drift in the radial direction that drives heavier particles out and the other in. The characteristic time describing the mobility drift toward the plasma edge is much longer than the effective interspecies collisional time  $\tau_{ie}$  by the ratio  $(\Omega_{ci}/\omega_R)^2$  [2]. The mass separation was clearly observed in  $e^-/\bar{p}$  plasma experiments [3, 4], apparently with a rate set by the cyclotron cooling time scale [3], which is too fast (by several orders of magnitude) comparing it to predictions of the separation rate based on the collisional drag diffusion/mobility theory [5] or the test particle calculations [2]. Thus, it appears that some other processes than collisional drag are responsible for the accelerated centrifugal mass separation.

Here we study the effects of omnipresent diocotron modes on the dynamics of the  $e^-/H^-$  plasma. These experiments were done on the CamV electron plasma apparatus at magnetic field  $B = 12 \text{ kG}$ , plasma column length  $L \approx 34 \text{ cm}$  and radius  $R_p \approx 1.2 \text{ cm}$ , electron density  $n_e \sim 10^7 \text{ cm}^{-3}$ . The detail apparatus description and typical electron plasma and trap parameters may be found elsewhere [6–8].

## $e^-/H^-$ PLASMA PRODUCTION

In our experiment negative hydrogen ions are produced and confined in a room-temperature electron plasma [9]. The  $H^-$  ions are formed in the plasma volume by dissociative electron attachment (DEA)



of low energy electrons onto vibrationally( $v$ ) and rotationally( $J$ ) excited hydrogen molecules [10]. Wide spectrum of ro-vibrationally excited molecules  $H_2(v_i, J_i)$  is generated in the recombinative desorption process of atomic hydrogen on the trap electrode and wall surfaces [11]. The  $H^-$  yield strongly depends on the electrodes temperature, and some conditioning of the electrodes by heating and/or positive hydrogen ion bombardment leads to an enhanced recombinative desorption, resulting in a significantly increased in-volume  $H^-$  production rate. Since the total  $H^-$  yield is proportional to the number of confined electrons  $Q_e$ , we characterize the ion production (electron conversion) rate as  $p_{H^-} \equiv d(Q_{H^-}/Q_e)/dt$ . In our best vacuum conditions ( $P_{H_2} \leq 10^{-10}$  Torr) the  $H^-$  production rate saturates at the level  $p_{H^-} \sim 10^{-3}/sec$  after 48 hours of the trap's electrodes heating (conditioning) by thermal radiation from the hot tungsten filament. This rate allows one to accumulate the charge fraction of  $H^-$  ions up to 20% in about 200 sec plasma confinement time. It is instructive to note here that the DEA process conserves the total plasma charge  $Q(t)$ , i.e.,  $Q(t) \equiv Q_e(t) + Q_{H^-}(t) = Q_e(0)$ .

## DIAGNOSTIC TECHNIQUES

Measurements of the diocotron and plasma frequencies is an attractive way to monitor the different mass fractions, since the frequencies can be measured with high precision, and the entire evolution can be reconstructed from one experimental cycle. Neglecting for a moment the temperature dependence, one can state that frequency of the primary ( $m_\theta = 1$ ) diocotron mode,  $f_{1d}(t) \sim 2.3$  kHz, represents *the total (net) charge line density* of the plasma,  $eN_{qL}(t) \equiv [Q_e(t) + Q_{H^-}(t)]/L$ , as the both mass fractions evolve in the slow ( $E \times B$  drift) diocotron motion, and  $f_{1d}(t)/f_{1d}(0) \propto N_{qL}(t)/N_{qL}(0)$ . On the other side, frequency of the primary ( $m_\theta = 0, k_z = 1$ ) plasma (*Trivelpiece-Gould*) mode,  $f_{TG1}(t) \sim 2.9$  MHz, represents *the electron charge line density* of the plasma,  $eN_{eL}(t) \equiv Q_e(t)/L$ , as only the electrons participate in the fast plasma oscillations, and  $f_{TG1}(t)/f_{TG1}(0) \propto \sqrt{N_{eL}(t)/N_{eL}(0)}$ . Thus, after an initial plasma cooling by cyclotron radiation of electrons down to the wall temperature, the diocotron frequency remains nearly constant and independent of the  $H^-$  production (accumulation) rate  $p_{H^-}$  (as  $N_{qL}(t) = const$ ), while the *TG*-mode frequency follows the continuously decreasing electron fraction density as  $d(\ln f_{TG1})/dt = -0.5p_{H^-}$ .

The  $m_\theta = 1$  diocotron mode in electron plasma is neutrally stable (neglecting its interaction with the resistive wall), so in an ideal case a single mode can persist during the entire plasma evolution. The finite length diocotron mode frequency has a magnetron shift arising due to the electrostatic force and the thermal pressure of plasma column balanced by the end confinement voltages [12]:

$$f_{1d}(t) = \frac{ceN_{qL}}{\pi BR_w^2} \cdot \left\{ 1 + \frac{R_w}{L} \left[ 1.20 \left( \frac{1}{4} + \ln \frac{R_w}{R_p} + \frac{T}{e^2 N_{qL}} \right) - 0.671 \right] \right\}. \quad (2)$$

Here, if we assume that during an experimental evolution the total plasma charge  $Q(t) \equiv eN_{qL}L$  is conserved, then temporal frequency variations are inflicted only by changes in plasma temperature  $T(t)$  and/or characteristic plasma radius (the bulk transport)  $R_p(t)$ . It is instructive to keep in mind that these changes also vary  $L(t)$  and  $N_{qL}(t)$ , accordingly. For a typical plasma electrostatic energy,  $e^2 N_{qL} \sim 10$  eV, and the trap aspect ratio,  $R_w/L \approx 0.1$ , a 1 eV change in plasma temperature  $T(t)$  results in about 0.5% change in the diocotron frequency  $f_{1d}(t)$ .

The *TG* mode frequency is also temperature dependent through the thermal pressure term as

$$f_{TG1}(t) = \frac{1}{2L} \sqrt{\frac{2e^2 N_{eL}}{m_e} \ln \frac{R_w}{R_p}} \cdot \left\{ 1 + \frac{3}{4 \ln(R_w/R_p)} \frac{T}{e^2 N_{eL}} \right\}, \quad (3)$$

and the thermal correction here is much stronger ( $\times 20$ ) than the one in  $f_{1d}(T)$  since it is not multiplied by the small aspect ratio  $R_w/L$ .

In the end of a particular evolution, by dumping the plasma column axially onto the phosphor screen with a CCD camera sensitive only to the fast electron component, the remaining amount of electrons  $Q_e(t_{end})$  is verified and calibrated against the plasma mode frequency  $f_{TG1}(t)$ . If the electron dumping process is done in quick enough manner, the  $H^-$  ions have no time to escape the trap, and the diocotron mode frequency after the dump reflects the  $H^-$  charge  $Q_{H^-}(t_{end})$ .

In addition, at any given time  $t_*$  during the plasma evolution we can rapidly clear the plasma column of the accumulated  $H^-$  ions, using a unique  $H^-$  shaking technique briefly described below. This brings down the current total charge line density  $N_{qL}(t_*)$  to the electron line density  $N_{eL}(t_*)$ , and measurement of  $f_{1d}(t_*)$  determines the lost  $Q_{H^-}(t_*)$  as well. There is no significant change in  $f_{TG1}(t)$  during the clearing process, i.e., there are no noticeable losses or heating of electrons.

## EXPERIMENTAL RESULTS AND DISCUSSIONS

Figure 1 shows the measured decrease in  $f_{TG1}(t)$  as electrons are “converted” to  $H^-$  ions, for two different apparatus conditions. In the first case, the electron source filament was ON only for a couple of hours (before the experiment), and the  $H^-$  ions production rate was as low as  $p_{H^-} = -2 d(\ln f_{TG1})/dt \approx .19/ksec$ . In the second case, the filament was ON for more than 48 hours, which results in  $p_{H^-} \approx 1.2/ksec$ . Note that this second rate would give complete conversion of  $e^-$  to  $H^-$  in about 1000  $sec$ , if no loss process occurred.

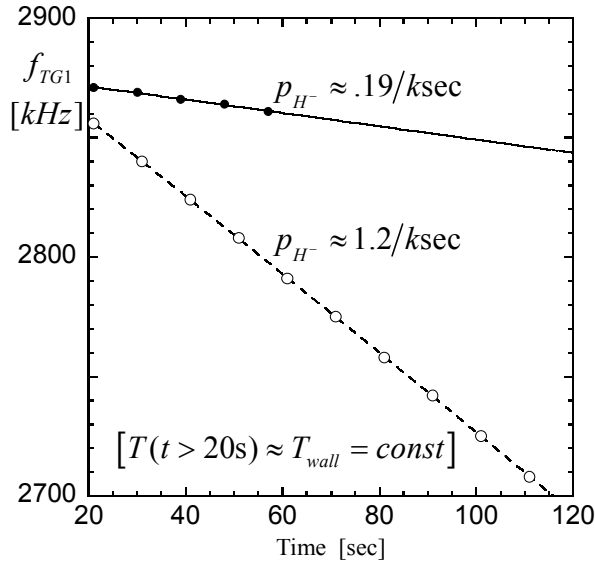


**FIGURE 1.** Measured frequency evolutions  $f_{TG1}(t)$  of thermally exited Trivelpiece-Gould modes for two extreme (low/high)  $H^-$  ion production rates. Only the late time parts of the  $f_{TG1}(t)$  evolutions ( $t > 20 sec$ , when  $T \approx T_{wall}$ ) are shown here.

For clearing the trapped  $H^-$  ions, the  $H^-$  shaking technique was developed. The longitudinal motion of the ions is caused by a small electric field internally generated by the mobile electron plasma as a result of variations in the wall potentials (the “sloshing column” motion) close to the ion “plasma frequency”  $f_{iTG} \sim \sqrt{m_e/M_i} f_{TG1}$ . Properly tuned (to keep the plasma length  $L(t) = const$ ) oscillations of the end confinement voltages shake plasma column back and forth axially ( $\Delta z \approx 1 cm$ ) at a resonant clearing frequency  $f_{cl} \approx 42 kHz \sim f_{iTG}$ . The full clearing cycle of accumulated  $H^-$  ions requires about 500 rounds (10  $msec$ ) of the plasma column shakings.

Figure 2 shows the diocotron mode amplitudes and frequencies as an injected electron plasma cools down to room temperature, exhibiting diocotron growth and damping. The weak diocotron growth is due to  $\sim 10 pA$  of transiting  $H_2^+$  ions [13], incidental to the trapped  $H^-$  ions effects considered here. The diocotron damping is due to accumulation and outward transport of  $H^-$  ions; and the damping ceases with application of “ $H^-$  clearing” steps.

Figure 2(a) shows examples of the  $f_{1d}(t)/f_{1d}(t_*) \propto N_L(t)/N_L(0)$  diocotron frequency evolution for small amplitude modes  $d(t) \equiv D/R_W \lesssim 10^{-2}$  excited right upon the electron plasma injection. After initial exponential cooling down as  $\Delta f_{1d}(t) \propto \Delta T e^{-t/\tau_c}$ , the diocotron frequency shows a very small decline rate as  $d(\ln f_{1d})/dt \leq 10^{-5}/sec$ , coming from the slow radial expansion (transport) of the electron plasma. Note that this decline rate is at least 20 times smaller than concurrent rate  $d(\ln f_{TG1})/dt = -0.5p_{H^-}$  (see Fig. 1). However, when we apply a train of  $H^-$  clearing cycles, the diocotron frequency drops down by the present fraction of  $H^-$  ions, matching the concurrent total charge line density  $N_{qL}(t_*)$  to the electron line density  $N_{eL}(t_*)$ .

Figure 2(b) shows evolutions of diocotron mode amplitudes corresponding to Fig. 2(a). With no ongoing  $H^-$  ion accumulation the diocotron mode growth first shows a slow exponential growth with an increment  $\gamma_+ \sim .05/sec$  defined by the single pass  $H_2^+$  ion-induced instability [13]. As the electron temperature cools down and the DEA process starts to convert electrons into  $H^-$  ions, the diocotron mode growth first shows a slowing down, and then ultimately turns into a damping. Even so, the (repetitive) plasma clearing of the  $H^-$  ions recovers the original exponential growth.

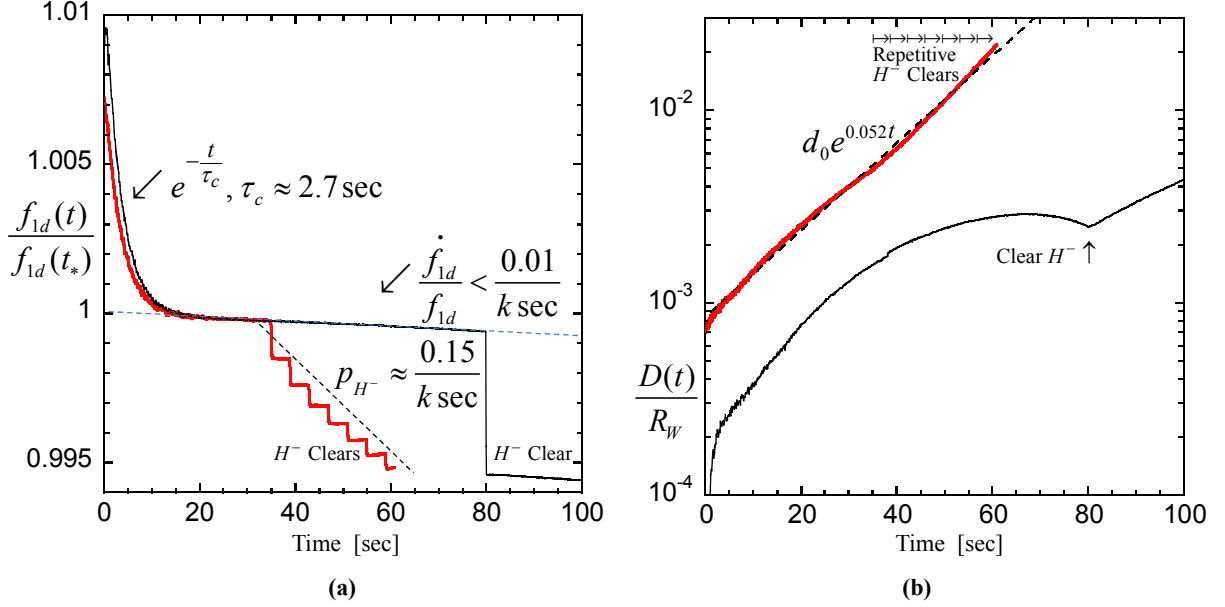


**FIGURE 2 (a, b).** Measured evolutions of (a) frequency  $f_{1d}(t)/f_{1d}(t_*)$  and (b) amplitude  $d(t) \equiv D/R_w \lesssim .01$  of diocotron modes for the slow  $H^-$  ion production rates,  $p_{H^-} \sim 0.1/ksec$ , with a variety of  $H^-$  clearing cycles. The bold (red) lines represent the case of seven consecutive  $H^-$  clearing cycles, and the thin (black) lines represent the case with only a single clearing cycle at  $t_* = 80 sec$ . Each clearing cycle adjusts the concurrent total charge line density  $N_{qL}(t_*)$  to the electron line density  $N_{eL}(t_*)$ .

Figures 3(a) and 3(b) illustrate diocotron mode evolutions observed in the case of high  $H^-$  ion production rates,  $p_{H^-} \sim 1/ksec$ . Here the modes are excited to moderate amplitudes  $d \sim 0.01$  to mitigate the stronger late stage damping. At this high  $H^-$  ion production rates the concurrent damping of diocotron modes becomes very potent ( $\gamma_H \gg \gamma_+ \cdot d$ ) and it clearly shows (see Fig. 3(b)) its *algebraic* character as  $d(t_* + \Delta t) \approx d_* - \gamma_H \Delta t$ , where  $\gamma_H \sim (2)p_{H^-}$ . The observed *algebraic* damping of diocotron mode is coincident with the accelerated downturn in  $f_{1d}(t)$  that reflects an increase of the plasma column mean-square radius  $\rho^2(t) \equiv \langle (r - r_{com})^2 \rangle$  relative to the center-of-mass (com) frame. When  $N_{qL}(t) = const$ , and  $T(t) \approx T_{wall} = const$ , the only change in the diocotron frequency  $f_{1d}(t)$  is set by (the net charge) plasma expansion as  $d(\ln f_{1d})/dt \approx -0.6(R_w/L) d(\ln \rho^2)/dt$  (see the magnetron term in Eq. (2)). We credit this change to a diocotron-induced centrifugal mass separation that by  $\vec{E} \times \vec{B}$  drifts moves uniformly produced in plasma volume  $H^-$  ions to the (radial) edge of the electron column. This outward flux of heavy charges “pushes back” on the diocotron displacement  $d(t)$ , thus conserving the mean-square radius of the total  $e^-/H^-$  charge ensemble in the center-of-cylinder frame (canonical angular momentum).

Figure 3(a) demonstrates that this accelerated radial transport in the total charge density (as the two pronounced downturns in the late time  $f_{1d}(t)/f_{1d}(t_*)$  evolution) is active only during the diocotron mode damping stages ( $t > 30 sec$ , and  $t > 70 sec$ ), i.e., when (1) the diocotron mode and (2) its algebraic damping are both present. There is no comparable fall in  $f_{1d}(t)$  when the diocotron mode is growing, and in the time span  $55sec < t < 70sec$  when the diocotron mode is damped away. This decline of the  $\ln(R_w/R_p)$  magnetron term in Eq. (2) then continues again following the external re-excitation of the diocotron mode. It is instructive to note that all three rates here (the  $H^-$  ion production rate  $p_{H^-} \sim 1/ksec$ , the diocotron damping rate  $\gamma_H \approx 1.9/ksec$ , and the radial transport rate  $d(\ln \rho^2)/dt \approx 1.6/ksec$ ) are meaningfully close to each other. Heating of the electron plasma above a few tenths of an eV seizes up both the diocotron damping and the ion production/separation processes.

The *algebraic* nature of this damping is more clearly shown in Fig. 3(b). At this time, the original ( $t = 0$ ) diocotron mode was already completely damped (after its initial exponential growth) by a fast  $H^-$  ion production (and separation) rate, so at  $t_* = 60 \text{ sec}$  the diocotron mode was re-excited. In addition to the linear slope,  $-\gamma_H \Delta t$ , the fitting curve in Fig. 3(b) also includes an exponentially vanishing “surplus  $H^-$  flux” term,  $\sigma \tau_s e^{-\Delta t / \tau_s}$ , to account for a surplus of  $H^-$  ions accumulated in the plasma volume during the preceding absence of the diocotron mode, i.e., before the diocotron-induced mass separation kicks in again. Derived from this fit the surplus loss (separation) time,  $\tau_s(d_*) \approx 0.3 \text{ sec}$ , is extremely fast compare to the collisional drag separation time,  $\tau_{ie} (\Omega_{ci} / \omega_R)^2 \sim 10^4 \text{ sec}$ , as well as to the top damping and ion production rates.

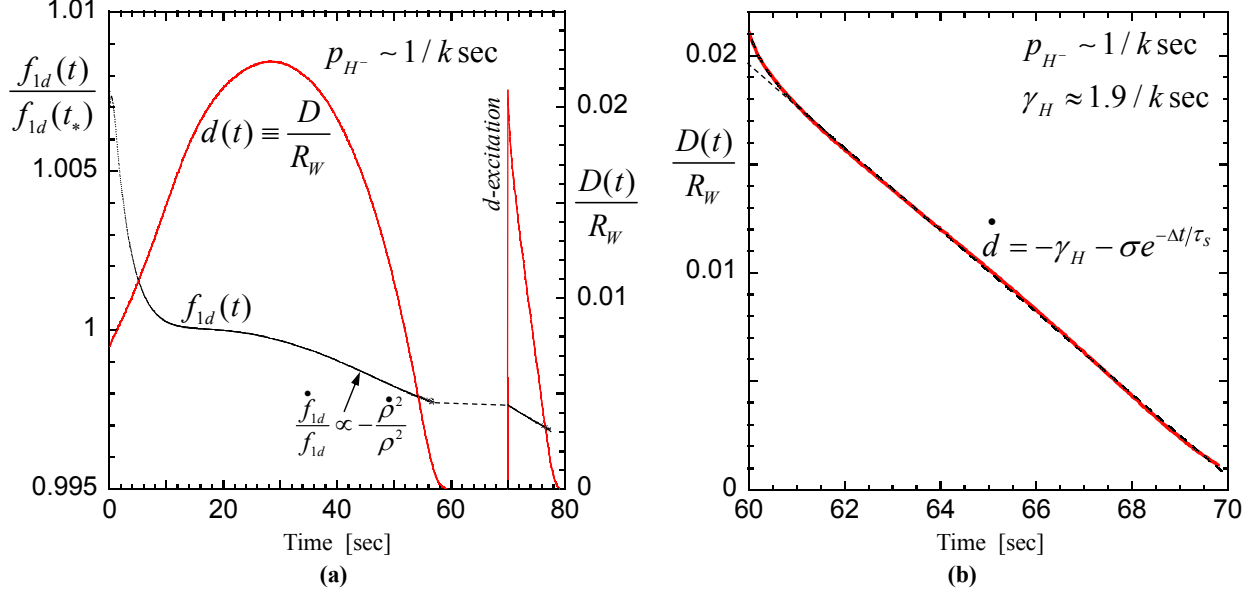


**FIGURE 3 (a, b).** Measured evolutions of the diocotron mode in the case of high  $H^-$  ion production rates,  $p_{H^-} \sim 1/ksec$ . (a) Frequency  $f_{1d}(t)/f_{1d}(t_*)$  and amplitude  $d(t) \equiv D/R_W$  with a strong late time damping,  $\gamma_H \approx 1.9/ksec$ . The damping is coincident with the accelerated downturn in  $f_{1d}(t)$  that reflects plasma expansion as  $d(\ln f_{1d})/dt \approx -0.6(R_W/L) d(\ln \rho^2)/dt$ . (b) Amplitude  $d(t)$  of the diocotron mode re-excited at  $t_* = 60 \text{ sec}$  on a fine time scale emphasizing the *algebraic* (non-exponential) character of the damping process, and also showing the effect of exponentially vanishing non-separated  $H^-$  “surplus” accumulated in the plasma volume during the absence of the diocotron-induced mass separation.

## SUMMARY

The ability to accumulate up to 20% charge fraction of  $H^-$  ions (in about 200 seconds) in room temperature cold electron plasma has been demonstrated in our experiments. The  $H^-$  ion accumulation process causes a novel *algebraic* damping of diocotron modes with the damping rates set by the ion production rate, and this damping is driven by the abnormally fast centrifugal mass separation (outward transport of the newly produced  $H^-$  ions in the “wobbling” electron plasma). Whereas all these rates are meaningfully close to each other, thus far no theoretical explanation has been given for the phenomenon. While the collisional drag centrifugal mass separation rates are admittedly slow in many applications, these rates can be greatly enhanced by the ubiquitous presence of diocotron modes discussed here.

## ACKNOWLEDGMENTS

This research was supported by NSF/DoE Partnership grants PHY-1414570 and DE-SC0002451.

## REFERENCES

1. T. M. O’Neil, Phys. Fluids **24**, 1447–1451 (1981).

2. M. Amoretti, C. Canali, C. Carraro, V. Lagomarsino, A. Odino, G. Testera, and S. Zavatarelli, *Phys. Plasmas* **13**, 012308 (2006).
3. G. B. Andresen *et al.* (ALPHA Collaboration), *Phys. Rev. Letters* **106**, 145001 (2011).
4. G. Gabrielse *et al.* (ATRAP Collaboration), *Phys. Rev. Letters* **105**, 213002 (2010).
5. D. H. E. Dubin, “Equilibrium and dynamics of multispecies nonneutral plasmas with a single sign of charge,” in *Non-Neutral Plasma Physics VIII*, AIP Conference Proceedings 1521, edited by X. Sarasola *et al.* (American Institute of Physics, Melville, NY, 2013), pp. 26-34.
6. A. A. Kabantsev, Yu. A. Tsidulko, and C. F. Driscoll, *Phys. Rev. Letters* **112**, 055003 (2014).
7. A. A. Kabantsev, C. Y. Chim, T. M. O’Neil, and C. F. Driscoll, *Phys. Rev. Letters* **112**, 115003 (2014).
8. A. A. Kabantsev, D. H. E. Dubin, C. F. Driscoll, and Yu. A. Tsidulko, *Phys. Rev. Letters* **105**, 205001 (2010).
9. A. A. Kabantsev and C. F. Driscoll, “*TG* wave autoresonant control of plasma temperature,” in *Non-Neutral Plasma Physics IX*, AIP Conference Proceedings 1668, edited by H. Himura *et al.* (American Institute of Physics, Melville, NY, 2015), p. 020002.
10. J. Horáček, M. Čížek, K. Houfek, P. Kolorenč, and W. Domcke, *Phys. Review A* **70**, 052712 (2004).
11. S. Markelj and I. Čadež, *The Journal of Chemical Physics* **134**, 124707 (2011).
12. K. S. Fine and C. F. Driscoll, *Phys. Plasmas* **5**, 601–607 (1998).
13. A. A. Kabantsev and C. F. Driscoll, *Review of scientific instruments* **75**(10), 3628–3630 (2004).